Dissipative optomechanical coupling between a single-wall carbon nanotube and a high-Q microcavity

Meng-Yuan Yan,* Hao-Kun Li, Yong-Chun Liu, Wei-Liang Jin, and Yun-Feng Xiao†
State Key Laboratory for Mesoscopic Physics and School of Physics, Peking University, Beijing 100871, People's Republic of China
(Received 29 April 2013; published 1 August 2013)

We theoretically investigate optomechanical coupling between a single-wall carbon nanotube and a high-Q whispering gallery microcavity. The anisotropy in the refractive index of the nanotube results in polarization-sensitive optomechanical coupling. Moreover, the band structure of the nanotube leads to a strong dependence of the coupling strength on wavelength. In particular, strong and pure dissipative coupling can be achieved at the absorption resonance frequency of the nanotube, and the single-photon coupling strength can exceed 10 kHz. This strong coupling induces dissipative cooling of the nanotube oscillation, and ground-state cooling can be achieved.

DOI: 10.1103/PhysRevA.88.023802 PACS number(s): 42.50.Wk, 03.67.−a, 42.50.Lc

I. INTRODUCTION

Interactions between optical fields and mechanical resonators have been developing rapidly [1,2]. This type of light-matter interaction allows the manipulation of mechanical and optical quantum states at the same time. On the one hand, ground-state cooling of the mechanical mode has been achieved with recent developments in nanofabrication [3], leading to intense studies on the generation and measurement of mechanical quantum states at the mesoscale [4–7], and recent developments are pushing the cooling limit forward while accelerating the cooling process [8,9]. On the other hand, the nonlinear optical response of microcavities due to the interaction with mechanical resonators has also been investigated recently. Nonlinear optical effects such as optomechanically induced transparency [10–12], four-wave mixing [13,14], and photon blockade [15,16] were analyzed, all of which are of central importance in both fundamental studies of nonlinear optics and applied fields such as quantum information processing [17,18] and various high-resolution sensing protocols [19].

There are two types of optomechanical coupling, the dispersive coupling, where the displacement of the mechanical resonator modulates the resonant frequency of the optical cavity, and the dissipative coupling, where the displacement of the mechanical resonator modulates the damping rate of the optical cavity. Recent studies have found that dissipative coupling can cool the mechanics at blue detuning, and is able to achieve ground-state cooling without the resolved sideband limit [20,21]. Moreover, when the strength of both types of coupling are properly tuned, the destructive interference allows the backaction to mimic a zero-temperature environment [21]. A recent study has also shown the application of dissipative coupling in particle sorting and speed rectification [22]. However, it is difficult to construct systems in which dissipative coupling dominates, since dispersive coupling is usually much stronger than dissipative coupling in traditional systems. Current proposals on this issue are limited to waveguide-cavity coupling [23] and the Michelson-Sagmac interferometer [20]. Here we propose an optomechanical system comprising a semiconducting carbon nanotube (CNT) and a whispering gallery mode (WGM) microcavity. CNTs have characteristic band structures and a strong reliance of polarizability on wavelength [24]. The variable refractive index and absorption of CNTs in the range from the near infrared to the ultraviolet open up a new toolbox for tunable dispersive and dissipative optomechanical coupling, and enable pure dissipative coupling at the absorption resonance frequency. Moreover, with the sensitivity of the CNT band structure and optical conductivity on the external static fields, it is possible either to manipulate the coupling by applying a static field, or to use the system as a sensitive detector. Experimentally, CNT-based mass sensors and strain sensors have been investigated [25,26], with the detection limit down to a proton's mass.

Previous investigations on CNTs in optomechanical systems mainly exploit the phonon-exciton coupling along with the photon-exciton interaction to produce optomechanical coupling [27,28]. This approach requires a strong static inhomogeneous electric field, and the coupling is dispersive. Here we investigate the coupling of CNTs to WGM microcavities, where distance-dependent polarization and absorption induces a strong tunable optomechanical interaction. CNT mechanical resonators are favorable for achieving the strong-coupling regime because of their ultrasmall weight and large zero-point fluctuation. The performance of dissipative cooling and heating is investigated and ground-state cooling can be achieved under cryogenic temperature.

This paper is organized as follows. In Sec. II, we introduce the optomechanical system, and present the mechanical eigenfrequency and electron band structure of the semiconducting zigzag carbon nanotube. Section III describes the frequency and linewidth modulation induced by the carbon nanotube, and the optomechanical coupling therein. Factors which determine the coupling strength, including the chiral index and length of the single-wall carbon nanotube (SWNT), pump frequency, and polarization, are discussed. The full quantum Hamiltonian for the optomechanical system is derived at the end of this section. In Sec. IV the dissipative optomechanical coupling is

*myyan@pku.edu.cn
†yfxiao@pku.edu.cn; www.phy.pku.edu.cn/∼yfxiao/index.html

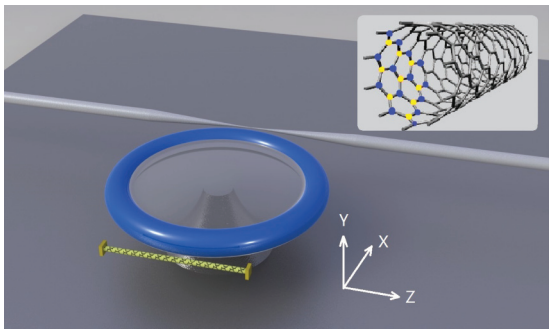

FIG. 1. (Color online) Schematic of the optomechanical system. Inset: Illustration of the CNT lattice. Yellow (light gray) and blue (dark gray) dots denote sublattices A and B, respectively.

applied to cool the nanotube. We demonstrate that ground-state cooling is achievable with a pump power of 10 mW.

II. MODEL

The proposed system consists of a microtoroid optical resonator and a single-wall carbon nanotube (SWNT), as shown in Fig. 1. The axis of the nanotube lies along the Z axis in the vicinity of the optical resonator. The microtoroid resonator has a major diameter of 20 μm and a minor diameter of around 3 μm, and the fundamental modes possess a quality factor on the order of 10^8. The SWNTs that we consider are semiconducting zigzag ones with a diameter below 1 nm. The mechanical flexural modes have frequencies ranging from 10 MHz to 1 GHz depending on the radius and length of the nanotube, as predicted by the classical beam model [29]

$$f_n = \frac{\beta_n^2}{4\pi}\frac{R}{L^2}\sqrt{\frac{E}{\rho}}, \tag{1}$$

where $\beta_1^2 = 22.37$, $\beta_2^2 = 61.74, \ldots$, R and L are the radius and length of the nanotube, $E = 1$ TPa is the Young's module, and $\rho = 2.2$ g/cm^3 is the density.

To obtain the optical properties of a SWNT, we need to investigate the SWNT electron band structure. A SWNT is a rolled-up single-layer graphene, in which each atom forms three σ bonds with its neighbors and keeps one electron unpaired. The unpaired electrons interact with each other to form a delocalized π orbital. Since the excitation energy is smaller for π electrons than for σ electrons, for an optical field in the visible and infrared regimes we can only take π electrons into consideration. Under a tight-binding approximation the Hamiltonian of π electrons in a SWNT can be expressed as [30]

$$H_0 = -\gamma_0 \sum_{i,j} (\alpha_i^\dagger \beta_j + \text{H.c.}), \tag{2}$$

where $\alpha_i^\dagger$, α_i, $\beta_j^\dagger$, and β_j are the creation and annihilation operators for electrons from sublattices A and B (yellow and blue dots in Fig. 1), respectively. The subscripts i and j refer to nearest neighbors. γ_0 is the electron hopping rate which characterizes the interaction strength between electrons, $\gamma_0 = 2.89$ eV.

The eigenfunctions of H_0 for valence and conductance bands, respectively, are denoted as $|\Psi_{\rm v}(\mu,k)\rangle$ and $|\Psi_{\rm c}(\mu,k)\rangle$,

$$|\Psi_{\rm c,v}(\mu,k)\rangle = C_{\rm A}^{\rm c,v}(\mu,k)\frac{1}{\sqrt{N}}\sum_{\mathbf{r_A}} e^{i\mathbf{k}\cdot\mathbf{r_A}} P_{\rm z}(\mathbf{r}-\mathbf{r_A}) + C_{\rm B}^{\rm c,v}(\mu,k)\frac{1}{\sqrt{N}}\sum_{\mathbf{r_B}} e^{i\mathbf{k}\cdot\mathbf{r_B}} P_{\rm z}(\mathbf{r}-\mathbf{r_B}), \tag{3}$$

where $\mathbf{k} = \mu\frac{2\pi}{na}\mathbf{e}_\theta + k\mathbf{e}_{\rm z}$ is the wave vector, $a = 0.246$ nm represents the length of the translation vector in graphene, n denotes the number of atoms in the circumference of the nanotube, and $\mu = -(n-1), -(n-2), \ldots, 0, \ldots, n$. $P_{\rm z}$ is the localized orbital for π electrons, N expresses the number of graphene unit cells in the nanotube, and $C_{\rm A}, C_{\rm B}$ are the coefficients in the expansion of the eigenstates. The corresponding eigenenergy for the conductance and valence bands, $E_{\rm c}$ and $E_{\rm v}$, are

$$E_{\rm c,v} = \pm\gamma_0 \left| \sum_{j=1}^{3} e^{i\mathbf{k}\cdot(\mathbf{r_{Bj}}-\mathbf{r_A})} \right|, \tag{4}$$

where B_j ($j = 1,2,3$) are the nearest neighbors of atom A.

III. CAVITY-NANOTUBE COUPLING

When the SWNT is positioned in the vicinity of a WGM optical cavity, it will be polarized by the optical field, and will modify the resonance frequency and linewidth of the optical cavity. This process is described by the semiclassical interaction Hamiltonian $H_{\rm i} = e\mathbf{r}\cdot\mathbf{E}$. Using the perturbation theory, the diagonal components of the susceptibility of the SWNT are [24]

$$\chi_{ii}(\omega) = \frac{2}{\varepsilon_0 V}\sum_{\mu',\mu,k',k} |\langle\Psi_{\rm c}(\mu',k')|e\mathbf{r_i}|\Psi_{\rm v}(\mu,k)\rangle|^2 \times \frac{E_{\rm cv}}{E_{\rm cv}^2 - (\hbar\Omega)^2}, \tag{5}$$

with $E_{\rm cv} = E_{\rm c}(\mu',k') - E_{\rm v}(\mu,k)$, $\Omega = \omega + i/\tau$, and $\tau \approx 10^{-13}$ s is the lifetime of electrons in the conductance band. ε_0 represents the vacuum permittivity and V the volume of the SWNT.

As the axis of the nanotube lies along the Z axis, the matrix element $\langle\Psi_{\rm c}(\mu',k')|z|\Psi_{\rm v}(\mu,k)\rangle$ is nonzero only when $\mu' = \mu$, and $\langle\Psi_{\rm c}(\mu',k')|x|\Psi_{\rm v}(\mu,k)\rangle$, $\langle\Psi_{\rm c}(\mu',k')|y|\Psi_{\rm v}(\mu,k)\rangle$ are nonzero only when $\mu' = \mu \pm 1$. This selection rule leads to the differences between $\chi_{zz}(\omega)$ and $\chi_{xx}(\omega)$, as shown in Fig. 2. The peaks correspond to resonances of the interband transitions, and their positions differ for χ_{zz} and χ_{xx}. The magnitude of $\chi_{xx}(\omega)$ is usually smaller than that of $\chi_{zz}(\omega)$ since the dipole moment $\langle\Psi_{\rm c}(\mu',k')|x|\Psi_{\rm v}(\mu,k)\rangle$ is generally smaller. Moreover, the real part of the susceptibility goes to zero at a wavelength that is slightly shorter than that at which the imaginary part reaches the maximum, and the tiny difference is proportional to the square of the electron decay rate $1/\tau$. At these points, we can realize pure dissipative coupling of the optomechanical system.

The polarization of SWNT will modulate the local electric field and will therefore alter the photon energy and lifetime. The resulting frequency shift and extra linewidth of the cavity

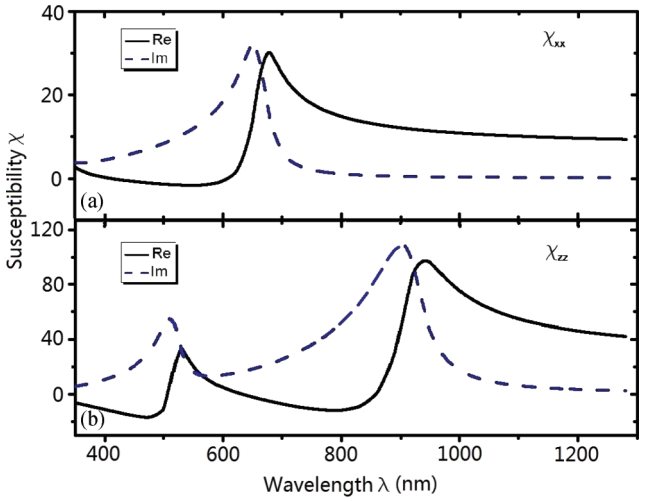

FIG. 2. (Color online) Real (black solid lines) and imaginary (blue dashed lines) parts of (a) $\chi_{xx}(\omega)$ and (b) $\chi_{zz}(\omega)$. The parameters are $\gamma_0 = 2.89$ eV and $\tau = 10^{-13}$ s.

mode can be expressed as

$$\Delta\omega + i\,\Delta\kappa = \frac{\omega_c}{2}\frac{\sum_i \int_V \varepsilon_0[\varepsilon_{r,ii}(\omega) - 1]|E_i(\mathbf{r})|^2 d\mathbf{r}}{\int_{V_0} \varepsilon|\mathbf{E}(\mathbf{r})|^2 d\mathbf{r}}, \quad (6)$$

where V_0 is the volume of the optical cavity. The real part corresponds to the frequency shift while the imaginary part corresponds to extra broadening of the line shape. The relation between the dielectric function ϵ and the susceptibility χ is [31]

$$\begin{aligned}\varepsilon_{r,zz}(\omega) &= 1 + \chi_{zz}(\omega),\\ \varepsilon_{r,xx}(\omega) &= 1 + \frac{\chi_{xx}(\omega)}{1 + \chi_{xx}(\omega)/2},\\ \varepsilon_{r,yy}(\omega) &= 1 + \frac{\chi_{yy}(\omega)}{1 + \chi_{yy}(\omega)/2}.\end{aligned} \quad (7)$$

It is different for parallel and perpendicular polarization because the screening effect is negligible for parallel polarization but not for the perpendicular case. The screened dielectric function $\varepsilon_{r,xx,yy}$ is almost a constant $\varepsilon_{r,xx,yy} \approx 3$ and is much smaller than $\varepsilon_{r,zz}$. As a result, the SWNT-cavity coupling depends on the polarization of the cavity mode. In the transverse electric (TE) mode, E_y dominates while the E_x and E_z components are negligible. Therefore, the contribution of $\varepsilon_{r,yy}$ plays the leading role, which means constant dispersive coupling, while in the transverse magnetic (TM) mode, E_x and E_z have approximately the same magnitude and E_y is much weaker. As $\varepsilon_{r,xx}$ is much smaller than $\varepsilon_{r,zz}$, we only need to take $\varepsilon_{r,zz}$ into consideration.

Since the susceptibility of SWNTs is irrelevant to tube length, the coupling between nanotubes and the microtoroid cavity will increase with tube length, because the interaction volume will be enlarged. When the tube is much shorter than the size of the cavity, the electric field around the nanotube can be treated as constant, thus $\Delta\omega$ and $\Delta\kappa$ will increase linearly with tube length. When the tube length is on the same order with, or much longer than, the major diameter of the cavity, the electric field decreases at the ends of the nanotube, and therefore the increase in $\Delta\omega$ and $\Delta\kappa$ slows down and approaches zero.

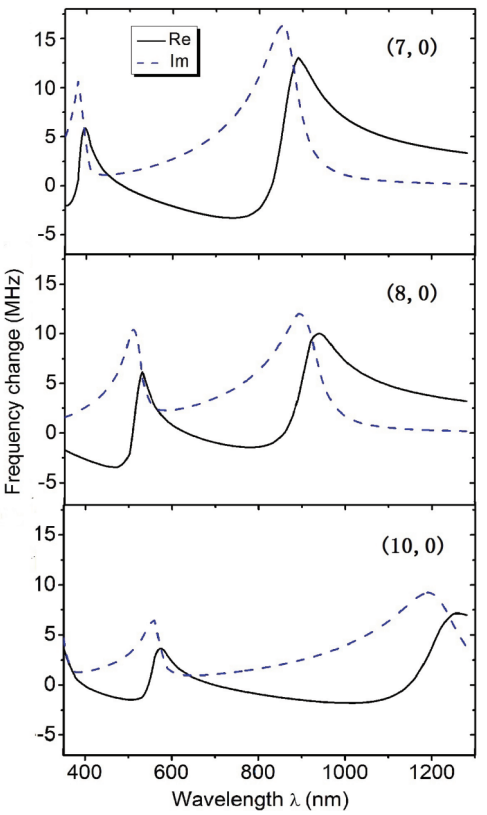

FIG. 3. (Color online) Frequency shift (black solid line) and extra linewidth (blue dashed line) of the optical mode coupled to SWNTs with chiral index (7,0), (8,0), (10,0), respectively. The length of the SWNTs is 1 μm. The distance between the SWNT and the microcavity is 30 nm.

A comparison of $\Delta\omega$ and $\Delta\kappa$ for a series of zigzag nanotubes is provided in Fig. 3. Nanotubes with different chiral indices possess different resonance peaks. For zigzag nanotubes $(n,0)$, the absorption resonance will generally redshift with increasing tube diameter. This can be explained by the nanotube band structure, as the band gap decreases with increasing chiral index. This special property of SWNTs allows for strong dissipative coupling in a wide range of wavelengths using different nanotubes in the SWNT family. In addition, when external fields are applied to modify the nanotube band structure, we can fine tune the coupling between the SWNT and the microcavity.

When we take the vibration of the SWNT into consideration, the frequency shift and extra linewidth depend on the displacement of the SWNT. We focus on the case of pure dissipative coupling between nanotubes and the cavity TM mode. This kind of coupling can be achieved when $\mathrm{Re}[\chi_{zz}(\omega)] = 0$ and the absorption is near its maximum (e.g., see the red arrow in Fig. 3). Due to the evanescent nature of the optical field outside the cavity, the field amplitude at the nanotube $E(x)$ decreases exponentially with its displacement x, $E(x) = E(0)\exp(-x/d_0)$. Therefore, qualitatively, the extra linewidth induced by the SWNT scales with $\exp(-2x/d_0)$.

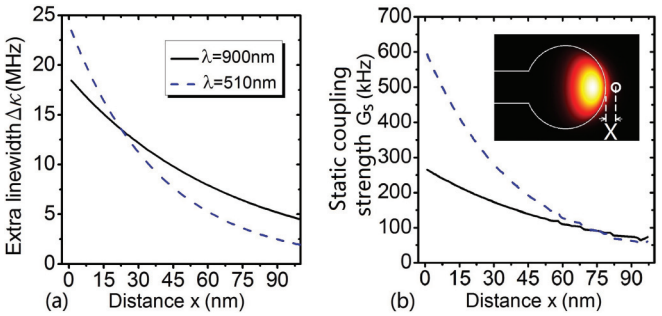

FIG. 4. (Color online) (a) Extra linewidth and (b) static coupling strength induced by distance-dependent SWNT absorption. SWNT chiral index (8,0), length $L = 1\ \mu$m. Microcavity major diameter $D = 20\ \mu$m, minor diameter $d = 2.7\ \mu$m. Inset: Illustration of the distance x.

The extra linewidth $\Delta\kappa$ and static coupling strength $G_s = |d(\Delta\kappa)/dx|$ for several dissipative coupling modes are shown in Fig. 4. Typically, at a distance $x = 15$ nm and wavelength $\lambda = 510$ nm, the coupling strength is $G_s \approx 0.4$ MHz/nm.

Realistically, each part of the SWNT will not have a uniform displacement due to clamping at the ends of the nanotube. Therefore, to be more quantitative, we need to consider the displacement field for the nanotubes' fundamental flexural mode, $U(l,t) = u_0(t)\cos(\pi l/L)$, where l is the coordinate along the nanotube's axis and L is the length of the nanotube. In this case the extra linewidth of the cavity mode is

$$\Delta\kappa = \frac{i\omega_c}{2}\frac{\mathrm{Im}[\chi_{ii}(\omega)]\varepsilon_0\pi R^2\int_{-L/2}^{L/2}|E_i(x+U(l,t))|^2 dl}{\varepsilon|\mathbf{E}_{\max}|^2 V_{\mathrm{cav}}} = \frac{i\omega_c}{2}\frac{\mathrm{Im}[\chi_{ii}(\omega)]\varepsilon_0 V}{\varepsilon|\mathbf{E}_{\max}|^2 V_{\mathrm{cav}}}\left[E_i\left(x+\frac{2}{\pi}u_0(t)\right)\right]^2. \quad (8)$$

Here $V_{\mathrm{cav}} = \int_{V_0}|\mathbf{Er}|^2 d\mathbf{r}/|\mathbf{E}_{\max}|^2$. Therefore the effective displacement for an oscillating nanotube is $\frac{2}{\pi}u_0(t)$, and the dynamic coupling coefficient is $G_d = d\Delta\kappa/du_0 = \frac{2}{\pi}G_s$. The single-photon coupling rate is given by $g_1 = x_0 G_d$, and $x_0 = \sqrt{2\hbar/m\omega_m}$ is the zero-point fluctuation. For a nanotube with chiral index (8,0) (diameter 0.63 nm) and length $L = 1\ \mu$m, the mechanical resonance frequency for the fundamental flexural mode is $\omega_m = 2\pi \times 12$ MHz, $m = 1.5\times10^{-6}$ pg, $x_0 = 43$ pm, thus achieving $g_1 \approx 11$ kHz at a distance of 15 nm and wavelength 510 nm.

Based on the above analysis we can derive the full quantum Hamiltonian for the optomechanical system. Under a TM-polarized field, the eigenstate of the free SWNT Hamiltonian $|\Psi_c(\mu,k)\rangle$ will couple selectively to the eigenstate $|\Psi_v(\mu,k)\rangle$. Therefore the semiclassical photon-electron interaction Hamiltonian $H_i = e\mathbf{r}\cdot\mathbf{E}$ is equivalent to

$$H_i = e\mathbf{E}(x)\sum_{\mu,k}\langle r(\mu,k)\rangle \times[|\Psi_c(\mu,k)\rangle\langle\Psi_v(\mu,k)| + |\Psi_v(\mu,k)\rangle\langle\Psi_c(\mu,k)|]. \quad (9)$$

We model each pair of eigenstates sharing the same wave vector as the ground state and excited state of a two-level atom, and define the operators $\sigma_\omega = |\Psi_v(\mu,k)\rangle\langle\Psi_c(\mu,k)$ and $\sigma_\omega^z = \frac{1}{2}[|\Psi_c(\mu,k)\rangle\langle\Psi_c(\mu,k)| - |\Psi_v(\mu,k)\rangle\langle\Psi_v(\mu,k)|]$, where $\omega = E_{cv}(\mu,k)/\hbar$. In addition, we quantize the optical field of the microcavity $\mathbf{E} = \frac{1}{2}[\hat{a}\mathbf{u}(r) + \hat{a}^\dagger\mathbf{u}^*(r)]$, and thus the Hamiltonian becomes $H_i = \sqrt{\kappa_\omega(x)}(a+a^\dagger)\sum_\omega(\sigma_\omega+\sigma_\omega^\dagger)$. Here we approximate the slowly varying function $r(\mu,k)$ as a constant, and κ_ω is only dependent on the SWNT displacement x. Expanding κ_ω to first order and retaining only the near-resonant processes, we obtain the full Hamiltonian for the optomechanical system, which also comprises the energy of optical field, mechanical oscillation, and electrons:

$$H = \omega_c a^\dagger a + \omega_m b^\dagger b + \sum\omega\sigma_\omega^z + \sum\sqrt{\kappa_\omega}(a^\dagger\sigma_\omega + \sigma_\omega^\dagger a)[1+g_\kappa(b+b^\dagger)] + \int\omega a_\omega^\dagger a d\omega + \sqrt{\kappa_c}\int(a_\omega^\dagger a + a_\omega a^\dagger), \quad (10)$$

where $b^\dagger$,b are the creation and annihilation operators of the SWNT mechanical mode, $g_\kappa = \frac{2}{\pi}\frac{1}{E}\frac{dE}{dx}\frac{x_0}{\sqrt{2}d_0} = \frac{2}{\pi}\frac{1}{\sqrt{2}}\frac{x_0}{d_0}$. The last term in the Hamiltonian describes the optical pumping. Since the relaxation rate of electrons in the carbon nanotube is around 10^{13} Hz [32], the pump light is usually not strong enough to change the population of electrons, i.e., $\sigma_\omega^z \approx -1/2$. Using the input-output formalism, which is similar to the perturbation theory approach taken above, the Hamiltonian can be simplified to

$$H = \omega_c a^\dagger a + \omega_m b^\dagger b + \sqrt{\kappa_c}(a_{\mathrm{in}}^\dagger a + a_{\mathrm{in}}a^\dagger) + \sqrt{\kappa_\omega}(a^\dagger\sigma_{\mathrm{in}} + \sigma_{\mathrm{in}}^\dagger a)[1+g_\kappa(b+b^\dagger)] - i\{\kappa_c + \tfrac{1}{2}\Delta\kappa_0[1+2g_\kappa(b+b^\dagger)]\}, \quad (11)$$

where $\Delta\kappa_0$ is the induced extra linewidth when the SWNT is at its static position, plotted in Fig. 4(a). $g_\kappa\Delta\kappa_0 = g_1$ is the single-photon coupling rate obtained earlier in this section. $a_{\mathrm{in}} = \int_0^\infty a_\omega(t=0)d\omega$ and $\sigma_{\mathrm{in}} = \int_0^\infty\sigma_\omega(t=0)d\omega$ are the pump light and electron coherence, respectively.

IV. DISSIPATIVE COOLING OF NANOTUBES

In the following, we explore the dissipative cooling of the nanotube. In the rotating frame, the Langevin equation of the optomechanical system can be written as

$$\dot{a} = -(i\delta+\kappa_c)a - i\sqrt{2\kappa_c}a_{\mathrm{in}} - i\sqrt{\kappa_\omega}\sigma_{\mathrm{in}}[1+g_\kappa(b+b^\dagger)] - \zeta a[1+2g_\kappa(b+b^\dagger)],$$
$$\dot{b} = -(i\omega_m+\gamma_m)b - i\sqrt{2\kappa_m}b_{\mathrm{in}} - ig_\kappa\sqrt{\kappa_\omega}(a^\dagger\sigma_{\mathrm{in}} + \sigma_{\mathrm{in}}^\dagger a). \quad (12)$$

Here $\zeta = \frac{1}{2}\Delta\kappa_0$. The steady-state solution of the intracavity field is

$$\bar{a} = \frac{-i\sqrt{2\kappa_c}\bar{a}_{\mathrm{in}} - i\sqrt{\kappa_\omega}\bar{\sigma}_{\mathrm{in}}}{i\delta - \kappa_c - \zeta}. \quad (13)$$

We extend this formalism by writing $a = \bar{a} + \delta a$, and after transforming the differential equation to the frequency domain, i.e., $a(\omega) = \int_{-\infty}^{+\infty}\delta a(t)e^{-i\omega t}dt$, Eq. (12) becomes

$$(i\delta - i\omega + \kappa_c + \zeta)a(\omega) = -i\sqrt{2\kappa_c}a_{\mathrm{in}}(\omega) - i\sqrt{\kappa_\omega}\sigma_{\mathrm{in}}(\omega) - i\sqrt{\kappa_\omega}\bar{\sigma}_{\mathrm{in}}g_\kappa[b(\omega)+b^\dagger(\omega)] - 2\zeta\bar{a}g_\kappa[b(\omega)+b^\dagger(\omega)],$$
$$(i\omega_m - i\omega + \gamma_m)b(\omega) = -i\sqrt{2\kappa_m}b_{\mathrm{in}}(\omega) - ix_0F(\omega),$$

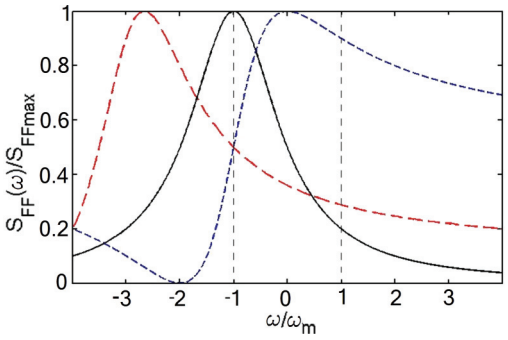

FIG. 5. (Color online) Force noise spectral density for pure dissipative or dispersive coupling. The black solid line corresponds to pure dispersive coupling with $\delta = -\omega_m, \kappa_c = \omega_m$, the short-dashed blue curve to pure dissipative coupling with $\delta = -\omega_m, \kappa_c = \omega_m$, and the long-dashed red curve to pure dissipative coupling with $\delta = -3\omega_m, \kappa_c = \omega_m$. Each spectrum has been scaled by its maximum.

$$F(\omega) = \frac{g_\kappa \sqrt{\kappa_\omega}}{x_0}[\bar{a}^* \sigma_{in}(\omega) + a^\dagger(\omega)\bar{\sigma}_{in} + \bar{a}\sigma_{in}^\dagger(\omega) + a(\omega)\bar{\sigma}_{in}^*]. \quad (14)$$

Here $F(\omega)$ is the backaction force on the nanotube, and the force noise spectrum $S_{FF}(\omega) = \langle F(\omega)F(-\omega)\rangle$ determines the damping and heating of the mechanics. When the optomechanical coupling is weak, the optically induced damping is given by $\gamma_o = x_0^2[S_{FF}(\omega) - S_{FF}(-\omega)]$. According to Eqs. (13) and (14), the force noise spectrum is

$$S_{FF}(\omega) = \frac{g_\kappa^2}{x_0^2}\left\{\frac{2\kappa_c\kappa_\omega}{(\omega-\delta)^2+\kappa_c'^2}|\bar{\sigma}_{in}|^2 + \frac{\kappa_\omega}{\delta^2+\kappa_c'^2}\left|\frac{i(\omega-2\delta)}{i(\omega-\delta)-\kappa_c'}\sqrt{\kappa_\omega}\bar{\sigma}_{in}^* + i\sqrt{2\kappa_c}\bar{a}_{in}^*\right|^2\right\}, \quad (15)$$

where $\kappa_c' = \kappa_c + \mathrm{Re}(\zeta)$. Since $|\bar{a}_{in}| \gg |\bar{\sigma}_{in}|$, the first term in the force noise spectrum can be omitted. The force noise spectrum shows a Fano-like line shape which is typical for a dissipative optomechanical coupling [21], as demonstrated in Fig. 5. Recall that $S_{FF}(\omega)$ is a simple Lorentzian for dispersive coupling, and this difference accounts for the cooling and heating regions shown in Fig. 6. At small detunings, $\gamma_o = x_0^2[S_{FF}(\omega_m) - S_{FF}(-\omega_m)]$ has opposite signs for the Fano-like line shape and Lorentzian line shape, thus dissipative coupling cools the mechanical oscillation at blue detuning, which is different from pure dispersive coupling. However, at large detunings $\delta > 2\omega$, the maximum of $S_{FF}(\omega)$ moves toward large $|\omega|$, as demonstrated by the red line in Fig. 5, and γ_o has the same sign as that of pure dispersive coupling, thus cooling occurs on the red detuned side.

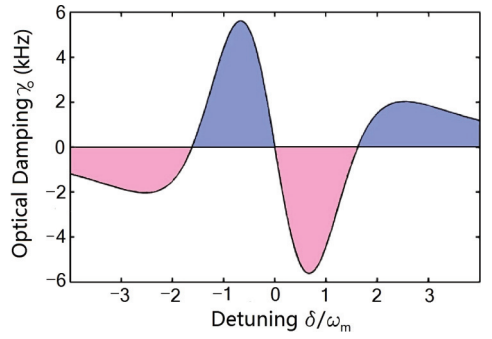

FIG. 6. (Color online) Optical damping as a function of detuning δ. The blue ($\gamma_o > 0$) and pink ($\gamma_o < 0$) areas correspond to cooling and heating, respectively. Input power $P = 5$ pW and other parameters are $g_\kappa = 1.77 \times 10^{-4}$, $[\zeta, \kappa_c, \omega_m, \gamma_m, \kappa_\omega] = [7.5\ \mathrm{MHz}, 1\ \mathrm{MHz}, 2\pi \times 12\ \mathrm{MHz}, 2\pi \times 80\ \mathrm{Hz}, 2.58 \times 10^{18}\ \mathrm{Hz}]$.

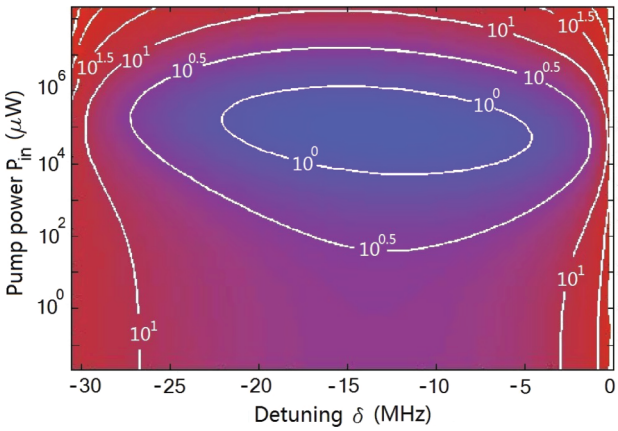

FIG. 7. (Color online) Steady-state phonon number as a function of detuning δ and pump power.

The steady-state phonon number can be termed as $n = (n_{th}\gamma_m + n_{opt}\gamma_o)/(\gamma_m + \gamma_o)$, where γ_o is the optical damping, and n_{opt} denotes the phonon number induced by the optical force. Under the condition $\sqrt{2\kappa_c}\bar{a}_{in} \gg \sqrt{\kappa_\omega}\bar{\sigma}_{in}$, the optical part can be derived and simplified to

$$n_{opt} = \frac{g_\kappa^2 2\kappa_c|\bar{a}_{in}|^2}{\gamma_o(\kappa_c'^2+\delta^2)}\kappa_\omega D, \quad (16)$$

where D denotes the density of states near the pump light frequency. For a 2-μm-long (8,0) SWNT at wavelength 510 nm, $D = 1.64 \times 10^{-13}\ \mathrm{Hz}^{-1}$. Other parameters in our system are $\zeta = 15$ MHz, $g_\kappa = 2.5 \times 10^{-4}$, $\kappa_c = 1$ MHz, $\omega_m = 2\pi \times 3$ MHz, $\gamma_m = 2\pi \times 20$ Hz [33], $\kappa_\omega = 2.58 \times 10^{18}$ Hz. Under cryogenic temperature $T_{env} = 0.15$ K, ground-state cooling can be achieved with a pump power of around 10 mW, as shown in Fig. 7. Under room temperature, the phonon number can also be greatly suppressed from n_{th} to several hundred.

In addition, the absolute value of optical damping at red detuning will be much larger than mechanical damping even with a pump power below $P = 1$ pW, resulting in regenerative oscillation. In this way we can explore the mechanical properties of nanotubes at the nonharmonic oscillation regime through its signature in the transmission of the optical cavity.

V. CONCLUSION

We have studied optomechanical coupling between a single-wall carbon nanotube and a WGM microcavity. The anisotropy in the polarizability and absorption of the nanotubes lead to polarization-sensitive optomechanical coupling. For the TE mode of the cavity, optomechanical coupling is approximately dispersive. For the TM mode, both dispersive and dissipative coupling can be realized, depending on the

pump wavelength. Since the ratio between these two kinds of coupling is tunable, various interference effects can arise in this system [21]. Particularly, pure dissipative coupling can be achieved at the absorption resonance frequencies, and the single-photon coupling strength is up to $g_1 = 11$ kHz. Dissipative cooling and heating of the nanotube oscillations are analyzed using linearized quantum Langevin equations. With a 2-μm-long (8,0) SWNT, ground-state cooling can be achieved, and regenerative oscillation can be achieved with a pump power well below 1 pW.

ACKNOWLEDGMENTS

This work was supported by the 973 program (2013CB328704), the NSFC (Grants No. 11004003, No. 11222440, and No. 11121091), and the Research Fund for the Doctoral Program of Higher Education (No. 20120001110068). M.Y.Y., H.K.L., and W.L.J. were supported by the National Fund for Fostering Talents of Basic Science (No. J1030310 and No. J1103205). M.Y.Y. and W.L.J. were supported by the National Undergraduate Innovational Experimentation Program.

[1] F. Marquardt and S. M. Girvin, Physics **2**, 40 (2009).
[2] M. Aspelmeyer, P. Meystre, and K. Schwab, Phys. Today **65** (7), 29 (2012).
[3] J. Chan, T. P. Mayer Alegre, A. H. Safavi-Naeini, J. T. Hill, A. Krause, S. Gröblacher, M. Aspelmeyer, and O. Painter, Nature (London) **478**, 89 (2011).
[4] O. Arcizet, P.F. Cohadon, T. Briant, M. Pinard, A. Heidmann, J. M. Mackowski, C. Michel, L. Pinard, O. Francais, and L. Rousseau, Phys. Rev. Lett. **97**, 133601 (2006).
[5] G. Anetsberger, O. Arcizet, Q. P. Unterreithmeier, R. Rivière, A. Schliesser, E. M. Weig, J. P. Kotthaus, and T. J. Kippenberg, Nat. Phys. **5**, 909 (2009).
[6] H.-X. Miao, S. Danilishin, H. Müller-Ebhardt, H. Rehbein, K. Somiya, and Y.-B. Chen, Phys. Rev. A **81**, 012114 (2010).
[7] J.-Q. Liao and C. K. Law, Phys. Rev. A **83**, 033820 (2011).
[8] Y.-C. Liu, Y.-F. Xiao, X.-S. Luan, and C. W. Wong, Phys. Rev. Lett. **110**, 153606 (2013).
[9] W.-J. Gu and G.-X. Li, Phys. Rev. A **87**, 025804 (2013).
[10] G. S. Agarwal and S. Huang, Phys. Rev. A **81**, 041803 (2010).
[11] S. Weis, R. Rivière, S. Deléglise, E. Gavartin, O. Arcizet, A. Schliesser, and T. J. Kippenberg, Science **330**, 1520 (2010).
[12] A. H. Safavi-Naeini, T. P. Mayer Alegre, J. Chan, M. Eichenfield, M. Winger, Q. Lin, J. T. Hill, D. E. Chang, and O. Painter, Nature (London) **472**, 69 (2011).
[13] H.-T. Tan and G.-X. Li, Phys. Rev. A **84**, 024301 (2011).
[14] S. Huang and G. S. Agarwal, Phys. Rev. A **81**, 033830 (2010).
[15] X.-X. Ren, H.-K. Li, M.-Y. Yan, Y.-C. Liu, Y.-F. Xiao, and Q. Gong, Phys. Rev. A **87**, 033807 (2013).
[16] P. Rabl, Phys. Rev. Lett. **107**, 063601 (2011).
[17] L. Tian and H. Wang, Phys. Rev. A **82**, 053806 (2010).
[18] D. Chang, A. H. Safari-Naeini, M. Hafezi, and O. Painter, New J. Phys. **13**, 023003 (2011).
[19] J.-J. Li and K.-D. Zhu, Appl. Phys. Lett. **101**, 141905 (2012).
[20] A. Xuereb, R. Schnabel, and K. Hammerer, Phys. Rev. Lett. **107**, 213604 (2011).
[21] F. Elste, S. M. Girvin, and A. A. Clerk, Phys. Rev. Lett. **102**, 207209 (2009).
[22] S. J. M. Habraken, W. Lechner, and P. Zoller, Phys. Rev. A **87**, 053808 (2013).
[23] M. Li, W. H. P. Pernice, and H. X. Tang, Phys. Rev. Lett. **103**, 223901 (2009).
[24] A. Zarifi and T. G. Pedersen, Phys. Rev. B **80**, 195422 (2009).
[25] J. Chaste, A. Eichler, J. Moser, G. Ceballos, R. Rurali, and A. Bachtold, Nat. Nanotechnol. **7**, 301 (2012).
[26] T. Yamada, Y. Hayamizu, Y. Yamamoto, Y. Yomogida, A. Lzadi-Najafabadi, D. N. Futaba, and K. Hata, Nat. Nanotechnol. **6**, 296 (2011).
[27] I. Wilson-Rae, C. Galland, W. Zwerger, and A. Imamoğlu, New J. Phys. **14**, 115003 (2012).
[28] J.-J. Li, C. Jiang, B. Chen, and K.-D. Zhu, J. Opt. Soc. Am. B **29**, 965 (2012).
[29] D. Garcia-Sanchez, A. San Paulo, M. J. Esplandiu, F. Perez-Murano, L. Forro, A. Aguasca, and A. Bachtold, Phys. Rev. Lett. **99**, 085501 (2007).
[30] S. Broadfoot, U. Dorner, and D. Jaksch, Phys. Rev. B **85**, 195455 (2012).
[31] L. X. Benedict, S. G. Louie, and M. L. Cohen, Phys. Rev. B **52**, 8541 (1995).
[32] D. Y. Joh, J. Kinder, L. H. Herman, S.-Y. Ju, M. A. Segal, J. N. Johnson, G. K.-L. Chan, and J. Park, Nat. Nanotechnol. **6**, 51 (2011).
[33] A. K. Hüttel, G. A. Steele, B. Witkamp, M. Poot, L. P. Kouwenhoven, and H. S. J. van der Zant, Nano Lett. **9**, 2547 (2009).